Coupling of Equipment Simulation and Feature-Scale Profile Simulation for Dry-Etching of Polysilicon Gate Lines

E. Baer, D. Kunder, P. Evanschitzky, J. Lorenz
Fraunhofer Institute for Integrated Systems and Device Technology IISB
Schottkystrasse 10, 91058 Erlangen, Germany
eberhard.baer@iisb.fraunhofer.de

***Abstract* — We demonstrate the coupling of plasma reactor equipment simulation and feature-scale profile simulation for dry etching of silicon in a chlorine plasma. Equipment simulation delivers fluxes of ions and neutrals, as well as the angular characteristics of the ions. These quantities are fed into a feature-scale simulator based on a Monte Carlo approach for determining relevant quantities on the feature surface, i.e. the concentration of adsorbed neutrals and the number of removed silicon atoms due to chemical sputtering. Using the coupled simulation system, we are able to study the influence of equipment parameters on the resulting etching profiles. As an example, we show the etching of polysilicon for gate formation and determine profile variations according to different positions on the wafer and according to varying bias applied to the substrate in the etching reactor.**

I. INTRODUCTION

The prediction of profiles and feature sizes of structures such as gate electrodes for transistors is an important part of the overall simulation chain spanning from the manufacturing process to the device. In this paper we employ our physical-based lithography and etching simulation to predict the shapes of gate electrodes etched in a chlorine plasma. To this end, the plasma chamber is simulated on equipment scale, and relevant quantities (fluxes of the different species and the angular characteristics of the ions) are delivered as input to feature-scale simulation. This allows us to link the operating conditions to the evolution of the profile on feature scale.

II. SIMULATION OF LITHOGRAPHY PRIOR TO ETCHING SIMULATION

As layout, an SRAM cell pattern on polysilicon level has been used, with a simple optical proximity correction method applied. The lithography simulation was performed with our simulation tool Dr.LiTHO [1]. Due to the small feature size, the mask diffraction spectrum has to be computed by using a rigorous electromagnetic field solver: For the simulations shown, the waveguide method [2] has been used as a rigorous field solver. The computation of the intensity distribution inside the resist is based on an extended Abbe approach. Finally, the resist profile is computed using a resist development model with a basic calibration. 193 nm water immersion with a strong off-axis illumination and unpolarized light were assumed. Dr.LiTHO provides the resist profile as a triangulated surface. To reduce the number of surface elements for the etching simulation, the footprint of the resist is extracted, smoothed and the 3D resist region is generated with steep sidewalls (Figure 1 shows one polysilicon line forming part of the SRAM layout). This geometry serves as input for the subsequent etching simulation. Our simulator is able to treat the problem in 3D. However, to study the effect of varying parameters on the etched profile, it is more efficient to simulate etching of a slice located at the position where, according to the SRAM layout, the gate electrode is above the active region.

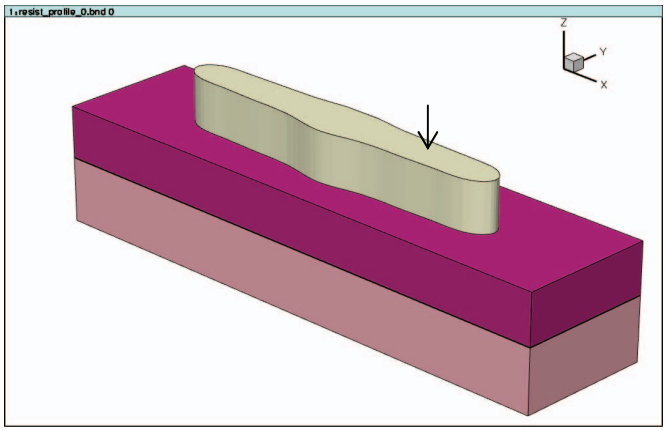

Figure 1. Resist geometry above polysilicon and gate oxide as obtained by physical-based lithography simulation using advanced models in the lithography simulator Dr.LiTHO. The slice position (slicing plane is perpendicular to x axis) for the subsequent etching simulation is marked by the arrow.

This work was supported by the Fraunhofer Internal Programs under Grant No. MAVO 817759 (HIESPANA).

III. EQUIPMENT SIMULATION OF PLASMA ETCHING REACTOR

For the etching of the transistor gate electrode, an inductively coupled plasma (ICP) reactor with chlorine chemistry is considered. An ICP model for a chlorine discharge was simulated with the program CFD-ACE+ [3], a multi-physics fluid code, to calculate the particle fluxes and the angular distribution of the ions at the wafer. For the chamber geometry, a DPS plus chamber of a Centura etcher (Applied Materials) was approximated by an axissymmetric geometry (see Figure 2). While this is reasonable for the four gas inlets, it cannot depict the asymmetry caused by the turbo pump. However, in this work, the focus was on the investigation of across-wafer variations in principle, assuming a dependence on the distance of the position under question to the center of the wafer only. Therefore effects leading to a deviation from this axissymmetry are not considered. This also allows a faster computation time and a better stability of the solver. In the chosen reactor setup, the coils to generate the magnetic field are above a ceramic dome. The lower electrode is biased with a RF voltage.

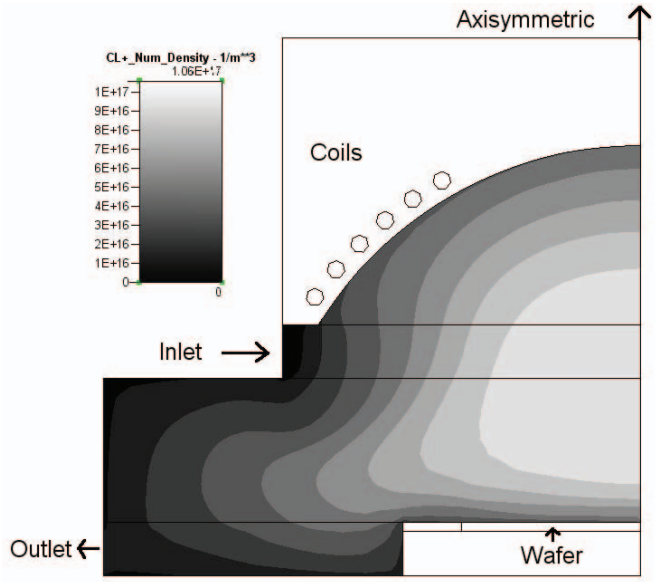

Figure 2. Simulated distribution of Cl^+ number density in a Centura plasma chamber. A cross section of the plasma chamber is shown with the rotational axis on the right. In the simulation, the conditions were a chamber pressure of 1 Pa, an inductive power of 1000 W, a Cl_2 flow rate of 100 sccm, and a bias voltage of 200 V.

In the computer model, the axis-symmetric geometry was discretized by a combination of an unstructured and a structured grid. A finer grid was used between the dome and the wafer to calculate the particle fluxes with higher accuracy. In the plasma, Cl_2, Cl, Cl^-, Cl^+, Cl_2^+, and electrons are considered. The gas phase reactions for a chlorine plasma were taken from the literature [4]. They describe heavy particle reactions including charge exchange and electron impact reactions leading to dissociation and ionization. The surface reactions at the wafer and the chamber walls are assumed to be recombination of Cl radicals and neutralization of ions.

Along the wafer, the fluxes of ions and neutrals and the angular distribution of the ions were calculated for different gas pressures, inductive powers, and bias voltages. The chlorine flow rate was 100 sccm in all simulations. For illustration, a cross section of the chamber is shown in Figure 2 with the distribution of the number density of Cl^+ ions.

IV. FEATURE-SCALE SIMULATION OF POLYSILICON ETCHING

The etching simulation on feature-scale level assumes radicals (in our case chlorine atoms) arriving at the surface with an isotropic angular distribution. Furthermore, ions (Cl^+ and Cl_2^+) with a directional angular characteristic impinge onto the surface. The radicals are adsorbed at the open silicon surface sites forming $SiCl_4$ which can leave the surface under bombardment of the ions. The ratio of emitted Si atoms per incident ion resulting from this mechanism is the so-called chemical sputtering yield (denoted by Y_{Si}).

We have set up equations for the local fluxes on the feature surface for ions and neutrals which determine the local etch rate. To this end, we discretize our surface by triangular facets and consider different events corresponding to the arrival of single particles (which could be real ones or pseudo particles) at the triangular facets. We have to distinguish between an arriving neutral and an arriving ion. In the current implementation of our model, we do not distinguish between the different sorts of neutrals and ions, but lump the neutral and ionic fluxes together into a single value each. We introduce the fraction of surface adsorption sites on the silicon surface covered by the neutrals as c_n. We normalize c_n in such a way that a value of 1 corresponds to complete coverage, i.e. each silicon surface atom is bond to 4 Cl atoms. A is the area of the triangle hit by the particle under consideration and σ_{Si} the surface site density of silicon (which is equal to $6.8 \cdot 10^{14}$ cm^{-2}). The number of bonds of a silicon surface atom for forming the reaction product is denoted by x_n. In our case, as mentioned above, as we assume $SiCl_4$ being the dominant etch product, x_n is set to 4. The etch rate is determined by the number of silicon atoms removed by the ion-enhanced desorption (called chemical sputtering) of the etch product $SiCl_4$. This number is normalized with respect to the number of silicon atoms in the top layer within the surface area corresponding to the triangle considered and is denoted by c_{etch}. We assume constant values for c_n and c_{etch} within each triangle. This means that all particle-related events act on the respective triangle as a whole.

The probability for a neutral particle to be adsorbed on the surface is proportional to the uncovered surface fraction ($1 - c_n$) corresponding to the open silicon surface sites. For a neutral particle hitting the surface at a triangle with an area A, we therefore can determine the changes of c_n and c_{etch} according to

$$\Delta c_n = \frac{1}{x_n A \sigma_{Si}} s_n \, (1 - c_n) \, n_{phys} \tag{1}$$

$$\Delta c_{etch} = 0 \tag{2}$$

The chemical sputtering due to the impinging ions affects the silicon atoms which have formed the reaction product with the Cl atoms. For an ion hitting the triangle we therefore obtain

$$\Delta c_n = -\frac{1}{A\sigma_{Si}} c_n \; Y_{Si} \, n_{phys} \tag{3}$$

$$\Delta c_{etch} = \frac{1}{A\sigma_{Si}} c_n \; Y_{Si} \, n_{phys} \tag{4}$$

In (1) – (4), n_{phys} is the number of real particles corresponding to a simulation pseudo particle. For the sticking coefficient s_n of the chlorine neutrals a value of 0.55 is assumed, and the chemical sputtering yield Y_{Si} is set to 3 [5]. The equations are solved on the surface grid using a Monte Carlo approach: Neutral and ionic pseudo particles are launched from above the structure according to the fluxes determined by equipment simulation, and, in case of the ions, according to the angular distribution obtained also from equipment simulation. The "size" of the pseudo particles n_{phys} is chosen in a way that during the Monte Carlo simulation a dynamic equilibrium for the concentration values c_n on the triangles is reached. The number of pseudo particles needs to be chosen according to the statistical error which can be accepted for the simulation results. This number needs to be adapted to the number of triangles.

We divide our simulation run into a number of time steps. In other words, we do not move the surface after each hitting pseudo particle but we sum up the concentration c_{etch} for a certain fraction of the etching time period and the surface is moved according to this concentration for this time period. In contrast to our previous work on etching, e.g. [6], we do not need to prescribe the thickness etched in planar sections (1D etched thickness), but we determine the thickness depending on the etching time specified and the neutral and ion flux values obtained from the equipment simulation.

For the simulations shown below, the total etching time period is divided into 15 time steps, the number of pseudo particles was calculated as 2000 times the number of surface triangles.

TABLE I.
RESULTS OF THE EQUIPMENT SIMULATION FOR AN OPERATING PRESSURE OF 1.5 PA, AN INDUCTIVE POWER OF 1500 W, AND A SUBSTRATE BIAS OF 200 V. THE STANDARD DEVIATION OF THE GAUSSIAN DISTRIBUTION DESCRIBING THE ANGULAR CHARACTERISTICS OF THE IONS IMPINGING ONTO THE WAFER IS 0.04 (RADIAN) FOR ALL POSITIONS ON THE WAFER.

Position from center of wafer [cm]	**Ion flux [10^{16} cm^{-2}]**	**Radical flux [10^{16} cm^{-2}]**
0.14	3.94	326
5.2	3.75	324
9.7	3.26	319

V. SIMULATION RESULTS

The input data needed for the feature-scale simulation are the fluxes of ions and radicals, and the angular distribution of the ions. The fluxes of neutrals and ions vary across the wafer, the standard deviation of the Gaussian distribution (representing the angular characteristics) does not. Furthermore, it turned out that the fluxes of ions and neutrals do not depend on the bias voltage. As an example, in Table 1 the values of the fluxes are listed for an operating pressure of 1.5 Pa, an inductive power of 1500 W, and a substrate bias of 200 V. Both ion flux and neutral flux decrease when the feature position changes from the center of the wafer to the rim. The relative change of the ion flux is larger than the relative change of the neutral flux. In consequence, the ratio between ion and neutral flux changes when the feature position changes from the center of the wafer to the rim.

The shape of the etched gate electrode is to a large extent governed by the overetch time, i.e. the etching time after the etch front has reached the gate oxide. Due to technological constraints, it is difficult to achieve a selectivity between polysilicon and oxide of larger than 30 [7]. In consequence, this constraint poses a limit for the overetch time. For different positions on the wafer, we find different etch rates with the etch rate being largest in the center of the wafer. We adjusted the etch time to such a value, that for this maximum etch rate half of the gate oxide thickness (i.e. 0.6 nm of a total thickness of 1.2 nm) is consumed during the overetch, assuming a selectivity between polysilicon and oxide of 30. For this etch time, the variations of the etch rate across the wafer lead to different etch profiles of the gate electrode, in particular to varying values of the critical dimension (CD). Cross sections of the etched gate electrode for different positions on the wafer are shown in Figure 3 and Figure 4, respectively. Here the etch time has been chosen as described above and the operating conditions where chosen as listed in Table 1.

The varying fluxes mainly affect the etched depth whereas almost no influence is visible on the tapering of the sidewall. The tapering is governed by the angular characteristics of the ions. The angular characteristic is mainly determined by the substrate bias voltage. It can be seen as a self-limiting effect: Once the tapering has reached a value that prevents ions from impinging onto the sidewall, etching stops at all, as we do not have purely chemical etching (running without ions) for the system studied here.

To demonstrate the influence of the angular distribution of the ions on the resulting profile, we have simulated the etching process for the same conditions as listed in Table 1 for a position at the center of the wafer, except for the substrate bias which now was set to 50 V. For this substrate bias, the standard deviation of the Gaussian distribution describing the angular distribution of the ions is 0.08, as determined by equipment simulation. This standard deviation is higher than the value for a substrate bias of 200 V which was determined to be 0.04. This is due to the smaller momentum transfer (resulting from a smaller voltage drop) to the ions in the direction towards the substrate. As the lateral component of the momentum of the ions is not influenced by the substrate bias, this leads to a larger angular spread of the ions. The profile simulation result is shown in Figure 5 and needs to be compared to the profile shown in Figure 3. It is visible that the profile in Figure 5 shows an enhanced sidewall bowing when compared to the profile in Figure 3. This is caused by the wider angular distribution of the ion flux.

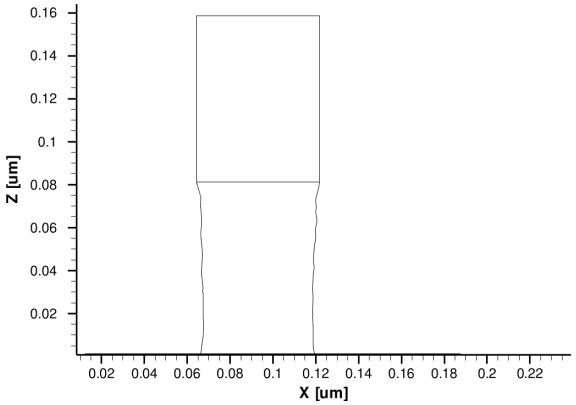

Figure 3. Profile simulation of gate etching for the operating conditions listed in Table 1. Position of the feature with a distance to the center of the wafer of 0.14 cm. The etching time was 6.5 s.

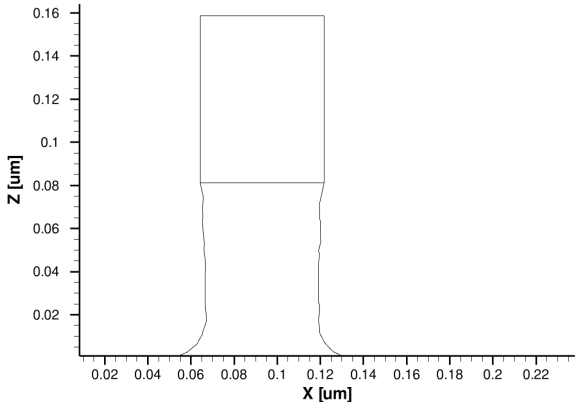

Figure 4. Profile simulation of gate etching for the operating conditions listed in Table 1. Position of the feature is almost at the rim of the wafer: The distance to the center is 9.7 cm. The etching time was 6.5 s.

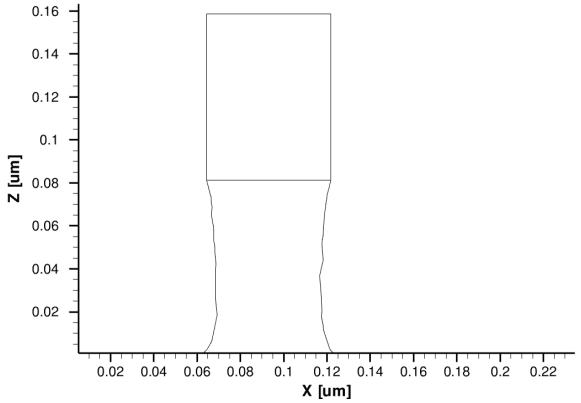

Figure 5. Profile simulation of gate etching for the operating conditions listed in Table 1, except for the substrate bias which is now set to 50 V. Position of the feature with a distance to the center of the wafer of 0.14 cm. The etching time was 6.5 s.

VI. Conclusions

We have demonstrated the coupling between lithography simulation, equipment plasma reactor simulation and feature-scale profile simulation for etching of polysilicon in chlorine-based chemistry. The fluxes of different species and the angular characteristics are transferred from equipment simulation to feature-scale simulation. Effects such as varying etch rates and sidewall bowing can be studied and correlated to equipment parameters.

Particularly regarding the effects at the surface, it is possible to model further mechanisms which may have an influence on the etching process, namely re-emission of neutrals, conversion of ions to neutrals with re-emission, or the re-adsorption of reaction products as passivating surface species. The Monte Carlo module employed for the simulation in principle offers the flexibility required for such extensions. However, one should keep in mind that an extension of the surface mechanisms usually will also require additional parameters that need to be determined (e.g. sticking coefficients of the different species adsorbed at the surface).

References

[1] T. Fühner, T. Schnattinger, G. Ardelean, A. Erdmann, "Dr.LiTHO - a development and research lithography simulator," Proc. SPIE, vol. 6520, pp. 65203F-1-65203F-12, 2007.

[2] P. Evanschitzky, A. Erdmann, "Fast near field simulation of optical and EUV masks using the waveguide method," Proc. SPIE, vol. 6533, pp. 65330Y-1-65330Y-12, 2007.

[3] Simulator CFD-ACE+, ESI Group, 2009.

[4] E. Meeks, P. Ho, A. Ting, R.J. Buss, "Simulations of $BCl_3/Cl_2/Ar$ plasmas with comparisons to diagnostic data," J. Vac. Sci. Technol., vol. A 16, pp. 2227-2239, July-August 1998.

[5] M. Tuda, K. Ono, K. Nishikawa, "Effects of etch producst and surface oxidation on profile evolution during electron cyclotron resonance plasma etching of poly-Si," J. Vac. Sci. Technol., vol. B 14, pp. 3291-3298, September-October 1996.

[6] E. Bär, J. Lorenz, H. Ryssel, "3D feature-scale simulation of sputter etching with coupling to equipment simulation," in: Simulation of Semiconductor Processes and Devices, G. Wachutka and G. Schrag, Eds., Wien New York: Springer, 2004, pp. 339-342.

[7] K.M. Chang, T.H. Yeh, S.W. Wang, C.H. Li, J.Y. Yang, "Dry etching of polysilicon with high selectivity using a chlorine-based plasma in an ECR reactor," Materials Chemistry and Physics, vol. 45, pp. 22-26, July 1996.